Electrodeposited Copper using Direct and Pulse Currents from Electrolytes Containing Low Concentration of Additives

Eden May Dela Pena, Sudipta Roy*

School of Chemical and Process Engineering, University of Strathclyde

James Weir Building, Glasgow, United Kingdom, G1 1XJ

*Corresponding author (sudipta.roy@strath.ac.uk)

Abstract

This work examines the effect of pulse deposition using a “lean” electrolyte, i.e., an acid-free bath with low cupric ion and additive concentrations using direct and pulse current. To this end, 25 μm copper films have been plated on stainless steel substrates from electrolytes containing only cupric ions, chloride and commercial additives. Films have been deposited from electrolytes containing different concentrations of additives ranging from 17% to 200% of the levels recommended by the supplier. The morphology of deposits was characterised using scanning electron microscopy and grain size has been determined using electron backscattered diffraction (EBSD). The crystalline structure has been examined using x-ray diffraction (XRD). It was found that although pulse currents or increasing amounts of chemical additive can reduce the grain size, the mechanisms for size reduction may be different. While current pulsing helps the generation of new nuclei, using additives suppresses grain growth. Mechanical and electrical measurements of these films showed that pulsing currents provide deposits with better mechanical and electrical properties. This has been attributed to lower number of defects when pulse currents are used. Our results also show that by using pulse currents, electrolytes containing low levels of additives and metal ions can be used to obtain copper deposits attaining industry specifications. Combining pulse currents with lean electrolytes may be therefore beneficial to the environment.

Keywords: electrodeposition, copper, additives, pulse plating, electrolytes, microfabrication

1.0 Introduction

Copper is the main material used to fabricate interconnects for electronic devices and in printed circuit boards (PCBs) [1, 2]. These industries typically require copper deposits to have certain attributes; in particular, low electrical resistance must be coupled with good mechanical properties [3]. Such specific properties are imparted by using electrodeposition processes where acid concentration and metal ions are prescribed through experience, which are typically 2.0 M H_2SO_4, and 0.6 M $CuSO_4$, respectively [4]. In addition, particular amounts of commercially available additives are also recommended by suppliers [4].

A recent advance in electrochemical mask-less patterning [5] process showed that micro-scale copper features, such as those required in PCBs, can be formed by dissolution [6] or deposition [7] using an acid-free, low copper ion concentration (0.1 M $CuSO_4$) electrolyte [8]. Their research also showed that lower concentrations of commercial plating additives could be added to improve deposit morphology and properties, so that they are suitable for industrial applications [9].

Indeed, using such "lean" electrolytes, i.e. acid-free, and containing low concentration of metal ions and additives can significantly reduce environmental impact of deposition processes [9, 10]. Although there have been investigations on metal recovery from rinse waters or spent electrolytes [11, 12] which contain low concentrations of metal ions and additives, but the quality of deposit is not important in those operations. Much less research has been carried out to determine if "lean" electrolytes can be used for plating high quality deposits which is the focus of the current paper.

One methodology that has been used to eliminate or lower additives in electrolytes is the use of pulsing currents [13] which has been applied successfully to plate chromium [14] and copper [15]. Whilst in direct current (DC) deposition a constant current is applied, in pulsed current (PC) deposition the applied current is switched on and off repeatedly [16].

Prior research has already shown that pulse currents can change grain size due to generation of new nuclei [17-19]. In addition, there is sufficient evidence that pulse currents can influence the action of levelling agents for higher levels of metal ion concentrations and additives [13, 20-23]. These earlier studies indicate that current modulation could become a significant factor in modification of deposit properties when metal ion and additive levels are low. This work aims to elucidate: (i) how the content of commercial additives influences the properties of pulse plated deposits from lean electrolytes; (ii) how do these two parameters interact when they are used in unison, and (iii) can pulse deposition be used to match industry specifications when low levels of metal ions and additives are used.

For this purpose, copper was deposited using direct and pulse currents (DC and PC). The additives used were Gleam A and B (Dow Chemical) which are typically used in PCB manufacturing. The lean electrolyte consisted of 0.1 M $CuSO_4$ and 17%, 33%, 50%, 100% and 200% of the additive concentration recommended by the supplier. In order to compare deposit properties obtained using these parameters, a standard deposition process using a solution of 0.63 M $CuSO_4$ with 2.0 M H_2SO_4 with recommended levels of additives (by supplier) was also used.

Copper films of 25 μm thickness were plated on polished dog-bone shaped steel substrates as per standards of the Institute of Interconnecting and Packaging Electronic Circuits (IPC) without agitation [24]. Deposit morphology of the films was examined using scanning electron microscope (SEM), and grain size and texture were determined using electron backscatter diffraction (EBSD). Crystal structure was ascertained by x-ray diffraction (XRD). The yield strength and resistivity of the foils were measured to compare against those recommended by IPC. Deposit properties are interpreted in terms of additive concentration and the mode of current applied. The findings were used to determine if pulse currents could be used to obtain deposit properties of industry standard using electrolytes containing low concentration of metals and addition agents.

2.0 Experimental

2.1 Plating Apparatus

Both direct current (DC) and pulsed current (PC) plating were performed using a classic two-electrode plating cell. The details of the plating system are described in a previous work [9]. Steel cathodes (308 grade) were manufactured to the specifications of IPC-TM-650 (IPC-TM stands for The Institute for Interconnecting and Packaging Electronic Circuits Testing Methods) standard [24]. A Cu rod (99.999% purity) was used as the anode. The anode-to-cathode area ratio was set at 2:1 to minimise polarisation at the anode. A Thurlby Thandar (PL-303) power supply was the DC source, while the Plating Electronics (PE86CB 3HE) pulse rectifier was the PC supply.

2.2 Chemicals and electrolytes

Electrolytes were prepared using technical grade $CuSO_4$, and when needed, H_2SO_4, (Sigma-Aldrich), and deionised water. The additives used were from a commercially available acid copper plating process (Copper Gleam™ HS-200, Dow Chemicals). The roles of the different additive components have been investigated and reported [25] in an earlier paper. Reiterating those findings, the component Copper Gleam HS–200 A is an accelerator, containing bis (sodiumsulfopropyl) disulphide (SPS) or its derivative mercaptopropane sulfonic acid (MPS). The component Copper Gleam HS–200 B is a suppressor, based on a high-molecular weight polyalkyl glycol compound such as polyethylene glycol (PEG).

These additives require the addition of a promoter, Cl^-, which was supplied using laboratory grade 37% HCl. It should be noted that the inclusion of HCl is in very low quantities, and is solely to enable additive action – it does not act as supporting electrolyte. Chemicals used for cleaning stainless steel (SS) substrates were concentrated HNO_3 and

ethanol (Sigma Aldrich). PRP200 photoresist (Electrolube) was used to insulate the back of the substrates. Table 1 lists the composition of the different plating electrolytes used in both DC and PC plating operation.

2.3 Plating Procedure

Prior to plating, the stainless steel substrates were dipped in concentrated nitric acid for 1 minute, and rinsed in deionised water for another minute. One side of the substrate was mechanically polished using silicon carbide sheets starting at grit #220 up to #4000 to obtain a mirror finish. The other side was insulated with photoresist to ensure that metal deposition occurred only on the one side. The exposed part of the substrate was swabbed with acetone for 30 seconds and air-dried at room temperature before it was immersed in the electrolyte for deposition.

Electrodeposition was carried out first using DC and then by PC mode to decouple the effect of additives from current modulation. Table 2 shows the plating parameters used in the DC plating experiments. Table 3 presents the plating parameters used in the PC plating runs. The choice of pulse parameters is more complex than DC ones, and a detailed description governing their choice is presented in section 3.0. As shown in the tables, for both DC and PC plating, the current was set at 40% of the corresponding limiting current. This current was chosen because it is well known that at this current density dendritic growth of deposit is unlikely. Plating efficiency for both current waveforms were determined from a separate set of experiments [25, 26], which are also included in the tables. In both cases the plating time was adjusted to ensure that the nominal thickness was the same.

In the deposition experiments, no mechanical stirring was employed and the total plating time was set to obtain a nominal film thickness of 25 μm. After the allotted plating time was reached, the substrate was removed from the solution, washed with deionised water

for 1 minute, wiped with lint free cloth, and left to dry in air. The plated Cu films were then carefully peeled off from the SS substrate, and were prepared for subsequent characterisation.

2.5 Characterisation

The plated specimens were subjected to different characterisation techniques: (i) SEM and EBSD (Hitachi SU-6600 EBSD system) to determine morphology, grain size and texture; (ii) XRD (PANalytical X'pert Pro) to assess crystal orientation, (iii) tensile test (Tinius Olsen H50KS) to determine mechanical properties; and (iv) four-point probe (Sigmatone Pro4) to analyse electrical properties. In order to carry out these analyses, a total of five films from each electrolyte were used. One film was used for the SEM, EBSD and XRD analysis. A second film was used to carry out the four-point probe test, and the remaining three were used for tensile tests.

For SEM, XRD and EBSD analysis, a 2×2 cm^2 area was cut out from the central portion of the Cu film. Grain size was determined using the software TANGO (HKL Technology A/S, 2001), which can be used to study EBSD orientation maps and extract crystallographic information. The grain structure map was obtained by adjusting band contrast (i.e. noise reduction and wild spikes extrapolation) to clearly reveal grains. The grain size parameter used is the major and minor axis of a fitted ellipse, and the software automatically measured the grain size based on the delineation of all of the grain boundaries.

For mechanical and electrical resistivity tests, a full film was used. Necessary care was taken to prevent damage on the Cu films, particularly during handling and specimen mounting which could compromise the quality of the mechanical tests. The tensile measurements followed ASTM-E345 [27], which is the standard for metallic films.

3.0 Determination of pulse parameters

Compared to DC plating, a simple pulse current wave-form has several variables that can influence deposit properties [13-15, 28-30]. Figure 1 shows a unipolar waveform together with important pulse parameters. The pulse on time, T_{on}, is the length of time the peak-current is applied, while the pulse off time, T_{off}, is the duration when the current is switched off. The sum of T_{on} and T_{off} is the total pulse period, T_p. Often, for convenience, the parameters are expressed using duty cycle, γ, and T_p which are related by:

$$\gamma = \frac{T_{\mathrm{on}}}{T_{\mathrm{p}}} \qquad \text{Equation 1}$$

The current imposed during the on-time is called the peak current density, i_p. The average current density for the entire pulse cycle, i_{ave}, in pulse plating, therefore, is given by:

$$i_{\mathrm{ave}} = i_{\mathrm{p}}\gamma \qquad \text{Equation 2}$$

In practice, it is desirable to maintain the mass flux for a pulse deposition process to be as close to the DC current condition in order to be able to compare their microstructures. Therefore, for any simple unipolar pulse deposition process, one needs to choose three independent parameters, T_p, γ and i_p.

During the application of a current pulse, the concentration boundary layer forms and relaxes as the current is switched on and off. Mass transfer during pulse deposition is described by a dual diffusion layer [31-33]; this consists of a pulsating inner diffusion layer and a stagnant outer diffusion layer. The calculation of the maximum operating peak current density, $i_{p,lim}$, is based on this dual diffusion layer model. The model states that the inner diffusion layer is influenced by pure diffusion and the off time, whilst the outer stagnant diffusion layer controls the overall plating which cannot exceed that obtained by DC plating [34, 35]. The pulse limiting current density, $i_{p,lim}$, is given by [36]:

$$\frac{i_{p,\lim}}{i_{d,\lim}} = \frac{1}{1-2\,T^{*}\cdot\sum_{m=1}^{\infty}\left[\exp(\lambda m)-1\right]} \qquad \text{Equation 3}$$

Where, $i_{d,\lim}$, is the DC limiting current density, T^* is a dimensionless pulse time given by DT_p/δ^2, where δ is the thickness of the outer diffusion layer and the summation term $\lambda_m = \pi^2 T^*(m - 1/2)^2$. Using the values of pulse time and γ used in this work, the ratio of the peak and DC limiting currents can be calculated. For example, for a T_{on} value of 100 ms and γ of 25% the ratio of $\frac{i_{p,\lim}}{i_{d,\lim}}$ is 3.3.

Since the experimental investigation of the whole range of γ, and T_p is impractical, a limited range of pulse parameters was explored. Initially the value of γ and T_p were set at "high" and "low" settings: a γ value of 25% and 50% and T_p value of 20 ms and 100 ms. The values of 25% and 20 ms represent waveforms of "short" on-times, and 50% and 100 ms represent "long" on-times for γ and T_p, respectively. It was found that all of the foils plated from the additive-free electrolytes and for T_p = 20 ms disintegrated, and some of those deposited T_p = 100 ms duration and γ = 50% tore partially. Since they could not be used for further characterisation, PC plating experiments focused on pulse parameters of T_p = 100 ms and γ = 25%.

Previous work on direct and pulse current deposition has shown that grain refinement is obtained when the peak current is high but well below mass transfer limitations [17-19, 30, 36]. The direct [9] and pulse limiting currents (as calculated from Equation 3) [26] are shown in Tables 2 and 3 for the electrolytes used in this study. Since the grain size for electrodeposited materials are dependent on approach towards mass transfer limit, similar mass flux conditions for DC and PC were maintained by choosing the applied plating current for both modes at 40% of their respective limiting currents. The approach towards mass transfer is characterised by two parameters, N_m and N_p [18, 38]

$$N_{\mathrm{m}} = \frac{i_{\mathrm{ave}}}{i_{\mathrm{d,lim}}}$$ Equation 4

$$N_{\mathrm{p}} = \frac{i_{\mathrm{p}}}{i_{\mathrm{p,lim}}}$$ Equation 5

where the different current densities are those referred to earlier in this section. Table 3 shows the calculated N_{m} and N_{p} for the pulse plating conditions used in the tests. Both values were constant and less than 1 in all settings (i.e. $N_{\mathrm{m}} = 0.33$ and $N_{\mathrm{p}} = 0.40$) to ensure that plating was carried out much below mass transfer limitations.

4.0 Results and Discussion

4.1 Morphology and grain size of deposits

SEM images (planar view) of PC plated products using a 0.1 M $CuSO_4$ solution containing different additive concentrations and a standard electrolyte are presented in Figure 2. The nomenclature used to describe the deposits follows a similar pattern used for electrolytes – for instance, "EP-50" is a sample which is pulse deposited from an electrolyte E-50. Overall, additive-free electrolytes provide coarse deposits either using 0.1 M $CuSO_4$ solution or that used in a standard electrolyte. Visual inspection of the images does not show a discernible difference in grain size or shape between the two baths. Increasing amounts of additive yielded deposits with increasing smoothness, as expected [17, 20-23, 37, 38]. Images of deposited copper plated using only 0.1 M $CuSO_4$ and standard solutions containing industry recommended levels of additives also appear very similar. When the deposits using pulse currents are compared against those obtained using DC published previously (see Figure S1), smoother deposits are observed for PC at lower additive concentrations. These results indicate that PC deposition can provide additional grain refinement over DC at low additive concentrations.

Electron back-scatter diffraction (EBSD) had to be used to determine grain size for the smooth deposits, which are shown in Figure 3. The grains are mainly equiaxed, with sizes significantly smaller than those obtained for additive free systems. Small nuclei, possibly due to re-nucleation during pulsing, are observed on top of Cu grains as the additive concentration is increased to 50% and above. However, the number of smaller grains in PC samples are fewer than those obtained using high additive levels (E-200) or standard electrolyte (S-100); this shows using additives generates more new nuclei through suppression of grain growth by adsorption at grain boundaries [37] than re-nucleation by current pulsing.

An interesting comparison is to assess if there is a difference in grain sizes between copper deposits in using pulse and direct current deposition. Figure 4 shows a comparison of the grain size of the PC as *vs.* DC (*cf.* S2) plated Cu for the different electrolytes. The grain size, as expected, is largest when no additive agents are used. In all additive containing electrolytes, the PC plated deposits have smaller grains than their DC plated counterparts. The reduction in grain size by the use of pulsing current is large in the absence of addition agents (72%) and shrinks to 22% when industry recommended levels are used. Qualitatively, one can conclude that grain refining effect of PC is more significant when additives are absent or are present at low concentrations. Interestingly grain sizes corresponding to those from a standard electrolyte can be attained when only 50% of additives are combined with pulsing currents.

4.2 Texture of Deposits

Using pulse currents can also change the texture of deposits. Figure 5 shows the XRD patterns for PC and DC deposited Cu, using 0.1 M $CuSO_4$ at different additive concentrations. In both plating modes, five prominent peaks with the corresponding diffraction planes were found in the XRD plots: (111), (200), and (220), (311) and (222). During DC deposition, the intensity of these peaks, especially those corresponding to (111), (200), and (220), increased

with increasing additive concentration. During PC deposition, in contrast, the intensity increased only up to an additive concentration level of 33% and stabilised thereafter.

Texture preference in the Cu films was assessed from the data in Figure 5 using the texture coefficient of the (hkl) plane, T_c(hkl) [39]:

$$T_c(hkl) = \frac{I(hkl)/I_o(hkl)}{\left(\frac{1}{n}\right)\sum_n I(hkl)/I_o(hkl)} \qquad \text{Equation 6}$$

where I(hkl) is the measured intensity of the chosen (hkl) plane, I_0(hkl) is the standard intensity of the plane (JCPDS data) and n is the number of diffraction peaks. The texture coefficient for the two strongest peaks corresponding to (111) and (200) were assessed, which are shown in Fig. 6.

In the absence of additives DC and PC textures are different, which shows that pulse deposition affects crystallisation when additives are absent. As shown in the figure, both (200) and (111) planes seem to be suppressed at low levels of additive; and the orientation for pulse and dc plated foils are similar. A slight preference for (111) orientation is observed at additive concentrations of 50% or higher. These results show that additive influence by adsorbing along preferred planes along grain boundaries continues even during pulse deposition.

4.3 Resistivity Measurements

Figure 7 show the resistivity of the DC and pulse plated films as a function of grain size in the 0.1 M $CuSO_4$ electrolyte. Note that the observed variation in grain size has been achieved by using different additive concentrations. As expected, the resistivity of the films increases with decreasing grain size for both the DC and pulse plating.

Theoretical descriptions of resistivity effects in polycrystalline materials assume that grain boundaries (along with other defects) induce electron scattering and thereby reduce the mobility of free electrons. Assuming that grain boundaries are the main cause of electron scattering, the Mayadas-Shatzkes model [40] describes the resistivity, ρ_G, for polycrystalline metals as:

$$\frac{\rho_G}{\rho_0} = \left[1 - \frac{2}{3}\alpha + 3\alpha^2 - 3\alpha^3 \ln(1 + \alpha^{-1})\right]^{-1} \qquad \text{Equation 7}$$

where ρ_0 is the bulk resistivity of the film, $\alpha = \frac{\lambda}{G}\frac{R}{1-R}$ is the scattering parameter, R is the material dependent grain boundary reflection coefficient, λ is the electron mean free path, and G is the grain size. For copper, λ = 39 nm and R typically has a value of between 0.20 and 0.80 [41, 42]. This equation can be fitted to the data in Figure 8 by assuming that ρ_0 corresponds to the measured resistivity values at the highest grain sizes, namely, ρ_0 = 2.0 μΩ cm for the PC plated copper films and ρ_0 = 2.15 μΩ cm for the DC deposited films. Assuming these ρ_0 values, the observed dependence of resistivity on grain size can be reasonably represented by assuming R = 0.7 - 0.8. It should be noted, however, that increase in resistance with decreasing grain size may arise from other factors; it may reflect increasing contamination of the films due to incorporation of organic additives. For example, a strong correlation between carbon contamination and resistivity in copper films has been previously found [43].

More interestingly, the resistivity of the PC plated films is lower than that for the DC plated films for a similar grain size. Whilst the actual reasons for the lower resistivity for PC samples is unclear at this point, it is feasible that the DC films contain higher quantities of impurities or defects. During pulse deposition, during the off time, it is possible that these may be minimised due to relaxation processes, even though the plating process is carried out at room temperature, resulting in an overall lower resistivity.

4.4 Mechanical Measurements

Figure 8 compares the mechanical properties; namely, (i) 0.2% offset yield strength (YS) (σ_y), (ii) ultimate tensile strength (UTS) (σ_f), and the (iii) ductility (ε_f) of the PC and DC-plated Cu films in 0.1 M $CuSO_4$ and the standard electrolyte. As expected, YS and UTS increase with increasing additive concentration due to a decrease in grain size, and correspondingly, ductility decreases. In all cases PC-plated deposits showed higher σ_y, σ_f due to their smaller grain size. However, the ductility for films obtained by pulse current plating, i.e. ε_f, are higher than the DC-plated deposits. Again higher ductility mirrors the findings of resistivity that indicate that there may be fewer defects in PC plated samples.

The changes in mechanical properties can be related to grain size by the classic Hall-Petch [44] relationship

$$\sigma_y = \sigma_i + \frac{k_y}{\sqrt{d}} \qquad \text{Equation 8}$$

where σ_y is the yield strength, d refers to the grain diameter and σ_i and k_y are material property constants. Figure 9 compares the yield strength of the DC and PC plated deposits using the against the theoretical yield strength as predicted by the Hall-Petch equation using $\sigma_i = 25$ MPa [45] and $k_y = 0.14$ MPa m$^{-1/2}$ [45] and the grain sizes shown in Figure 4. These data are in reasonable agreement with the findings of other work [46].

Pulse plated deposits are in reasonable agreement with equation 8, whereas DC plated deposits are significantly lower. Deposits obtained using direct current, on the other hand lie well below the theoretical curve, showing poorer mechanical strength, possibly due to defects. The good agreement of the PC plated films with Equation 8 support the findings that the PC deposition produces more compact and defect free films than those obtained by direct current deposition.

5.0 Discussion

Electrodeposition practitioners have used a variety of methods to control grain structure and orientation using non complexing aditives [17, 20, 47]. In this work we have examined the effect of a combination of additives, consisting of SPS (or MPS) and PEG which are known to adsorb on the surface of the electrode [25, 48]. Normally the adsorbed compounds are extremely difficult to detect ex-situ due to their low concentration in the electrolyte; however, there is evidence that Cu deposition from a solution containing SPS and PEG can lead to incorporation of impurities along grain boundaries [43, 48, 49].

Our findings consistently show that electrical resistivity, tensile strength and ductility are better for copper deposited by pulse currents, even when the grain sizes are smaller. When impurities are incorporated in a deposit, it would adversely affect these properties. It is possible that pulsing currents or potentials can allow desorption of these compounds from the surface during the off time [20, 21, 38] because their adsorption is potential dependent [37]. Recently our own group has carried out voltammetry using an electrochemical quartz crystal nano-balance, and have shown that fluoro-surfactant additives adsorb and desorb from copper surfaces depending on the applied potential [50].

In this regard, our findings show that whilst additive agents are more effective in suppressing grain growth by adsorbing at grain boundaries or particular planes, they can induce more impurities (or defects). Pulsing currents seem to provide a decrease in grain size via re-nucleation rather than by incorporation of impurities/defects and produce a more compact film. Indeed, our results show that it is possible to lower the content of additive agents using pulsing currents to achieve smaller grains, without detriment to deposit properties.

A second point to note that while both addition agents and current pulsing cause a reduction in grain size, there seem to be significant differences in their actions. Additive agents are more efficient is grain size reduction by adsorbing at grain boundaries, whereas pulse currents seem to reduce grain size by re-nucleation. The adsorption of additives along selected planes can change the orientation of the deposited material, which is observed in Figure 5, predominantly at low additive concentrations. For the case of copper, this results in a suppression of the (100), possibly because additives prefer to adsorb along these planes.

A challenge remains to determine if these deposits can attain electrical and mechanical properties specified by industrial needs, the properties of some PC and DC plated specimens are compared against IPC product standards in Table 5. The DC plated sample using 50% of the recommended value of additive concentration has slightly poorer performance as compared to the IPC standard; on the other hand, pulse plated samples using E-50 and E-33 electrolytes achieve the requirement. Using 33% of the industry recommended standards would not only provide better resistivity, strength and ductility, but also allow the use of an electrolyte containing lower metal ions, no acid and a lower additive concentration.

One concern of using lower metal ion concentration is that it can limit plating rates. As shown in Table 2 the plating rate of the standard electrolyte is four to five times higher than the lean electrolytes. In PCB manufacturing, plating rates of 1.5 - 2.0 ASD (15 - 20 $mA{\cdot}cm^{-2}$) are typically used. Improvements in plating rates can be achieved by increasing agitation.

5.0 Conclusion

Copper films of 25 μm thickness were electroplated using 0.1 M $CuSO_4$ with 0%, 17%, 33%, 50%, 100% and 200% of industry recommended additive concentrations using pulse current and direct current deposition. SEM and EBSD analysis showed that grain size

was reduced with increasing additive concentration or by pulsing currents. Whilst additives strongly suppressed grain growth by adsorption, pulse currents produced smaller grains via re-nucleation. XRD analysis showed that additives favoured the development of (111) texture in deposit by adsorbing at grain boundaries. Electrical resistivity for pulse deposited samples was smaller than DC plated deposits for the same grain size. Mechanical properties such as ductility and tensile strength for pulse current plated samples were also superior to those obtained by direct current.

This behaviour were interpreted as different mechanisms occurring during pulse current deposition; while additives decreased grain sizes by suppressing growth by adsorption along grain boundaries, pulse currents lowered grain sizes due to re-nucleation. Use of pulse current deposition in unison with additives in electrolytes can allow the addition agent to desorb during the off time, which can reduce the formation of defects in the deposit, leading to better mechanical and electrical properties. Finally, it was found that pulse current deposition could produce deposits which matched industry standards, showing that lean electrolytes could be used for industrial production which has environmental benefits.

Acknowledgement

Dr E.M. Dela-Pena acknowledges the support of ERDT-DOST scholarship through The University of the Philippines Diliman Quezon City. The authors acknowledge the support from Mesmoproc partners (www.mesmoproc.eu) in this work. Dr Todd Green is acknowledged for his contribution to section 4.3.

References

[1] P.C. Andricacos, C. Uzoh, J.O. Dukovic, J. Horkans, H. Deligiani, Damascene copper electroplating for chip interconnections, IBM J. Res. Dev. **42** (1998) 567-574.

[2] K. Kondo, R.N. Akolkar, D.P. Barkey, M. Yokoi, Copper Electrodeposition for Nanofabrication of Electronic Devices, Springer, New York, 2014.

[3] C.F. Coombs, Jr., Printed Circuits Handbook, sixth ed., McGraw Hill, New York, 2008.

[4] Product Datasheet for Copper Gleam HS-200 vertical acid copper for PWB metallization application, Dow Electronic Materials.

[5] S. Roy, Fabrication of micro- and nano-structured materials using mask-less processes, J. Phys. D: Appl. Phys. **40**(22) (2007) R413-R426.

[6] I. Schönenberger, S. Roy, Microscale pattern transfer without photolithography of substrates, Electrochim. Acta **51** (2005) 809-819.

[7] Q.-B. Wu, T.A. Green, S. Roy, Electrodeposition of microstructures using a patterned anode, Electrochem. Comm. **13** (2011) 1229-1232.

[8] S. Nouraei, S. Roy, Design of experiments in electrochemical microfabrication, Electrochim. Acta. **54** (2009) 2444-2449.

[9] E.M. Dela Pena, N. Bains, A. Hussain, A. Cobley, S. Roy, Effect of additive concentration during copper deposition using EnFACE electrolyte, Trans. IMF. **93**(6) (2015) 288-293.

[10] A. Vicenzo, P.L. Cavallotti, Copper electrodeposition from a pH 3 sulfate electrolyte, J. Appl. Electrochem., **32** (2002) 743-753.

[11] E.E. Farndon, S.A. Campbell, F.C. Walsh, Effect of Thiourea, Benzotriazole and 4,5-Dithiaoctane-1,8-Disulphonic Acid on the kinetics of copper deposition from dilute acid sulfate solutions, J. Appl. Electrochem. **25** (1995) 574-583.

[12]

[13] N. Ibl, J. Cl. Puippe, H Angerer, Electrocrystallisation in pulse electrolysis, Surf. Technol. **6** (1978) 287-300.

[14] P. Leisner, G. Bech-Neilsen, P Möller, Current efficiency and crystallization mechanism in pulse plating of hard chromium, J. Appl. Electrochem. **23** (1993) 1232-1236.

[15] P. Leisner, P. Möller, M. Fredenberg, I. Belov, Recent progress in pulse reversal plating of copper for electronics applications, Trans. IMF. **85**(1) (2007) 40-45.

[16] S. Roy, An overview of pulse plating in: W.E.G. Hansal, S. Roy, Eds. Pulse Plating, Eugen G. Lueze, Bad Saulgau, 2012, pp. 19-32.

[17] N. Imaz, E. Garcia-Lecina, C. Suarez, J.A. Diez, J. Rodriguez, J. Molina, V. Garcia-Navas, Influence of additives and plating parameters on morphology and mechanical properties of copper coatings obtained by pulse electrodeposition, Trans. IMF, **87**(2) (2009) 64-71.

[18] O. Chène, D. Landolt, The influence of mass transport on the deposit morphology and the current efficiency in pulse plating of copper, J. Appl. Electrochem. **19** (1989) 188-194.

[19] D. Landolt, General considerations concerning the influence of current form on metal, deposition, Oberfläsche-Surface, **25** (1984) 6-15.

[20] N. Tantavichet, M. Pritzker, Copper electrodeposition in sulphate solutions in the presence of benzotriazole, J. Appl. Electrochem. **36**(1) (2006) 49-61.

[21] S.S. Kruglikov, N.T. Kudriavstev, G.F. Vorobiova, A.Y. Antonov, On the mechanism of levelling by addition agents in electrodeposition of metals, Electrochim. Acta. **10** (1965) 253-261.

[22] H. Dyar, E.J. Taylor, J. Sun, M. Inman, P. Miller, A low cost semiconductor metallization /planarization process, Plat. Surf. Finish. **91** (2004) 32-44.

[23] M.S. Aroyo, Leveling in pulse plating with brighteners: synergistic effect of frequency and hydrodynamically active additives, Plat. Surf. Finish. **82** (1995) 53-57.

[24] IPC-TM-650 Test Methods Manual- TM 2.4.18B, IPC, Bannockburn, IL.

[25] E.M. Dela Pena, S. Roy, Electrochemical effect of copper gleam additives during copper electrodeposition, Trans. IMF. **95** (2017) 158-164.

[26] E.M. Dela Pena, Electrodeposition of copper using additive-containing low metal ion concentration electrolytes for Enface applications, PhD Thesis (2017) pp. 205-240.

[27] ASTM Standard E-345-16, Standard Test Methods of Tension Testing of Metallic Foil, ASTM International, West Conshohocken, PA.

[28] J.Cl. Puippe, N. Ibl, Influence of charge and discharge of electric double layer in pulse plating, J. Appl. Electrochem. **10** (1980) 775-784.

[29] J.Cl. Puippe, F. Leaman, Theory and Practice of Pulse Plating, American Electroplaters and Surface Finishers Society, Orlando, Florida, 1986.

[30] D. Landolt, A. Marlot, Microstructure and composition of pulse-plated metals and alloys, Surf. Coatings Technol. **169-170** (2003) 8-13.

[31] N. Ibl, Some theoretical aspects of pulse electrolysis, Surf. Technol. **10** (1980) 81-104.

[32] D. Landolt, M. Datta, Experimental investigation of mass transport in pulse plating, Surf Technol. **25** (1985) 97-110.

[33] S. Roy, Mass transfer consideration during pulse plating, Trans. IMF. **86**(2) (2008) 87-91.

[34] H.Y. Cheh, Electrodeposition of gold by pulsed current, J. Electrochem. Soc. **118** (1971) 551-557.

[35] D.T. Chin, Mass transfer and current-potential relation in pulse electrolysis, J. Electrochem. Soc. **130** (1983) 1657-1667.

[36] S. Roy, D. Landolt, Determination of the practical range of parameters during reverse-pulse current plating, J. Appl. Electrochem. **27** (1997) 299-307.

[37] L. Oniciu, L. Muresan, Some fundamental aspects of levelling and brightening in metal electrodeposition, J. Appl. Electrochem. **21** (1991) 565-574.

[38] L. Muresan, S. Varvara, Leveling and brightening mechanisms in metal electrodeposition, in: M. Nunez (Ed.), Metal Electrodeposition, Nova Science Publishers, New York, 2005, pp. 1-45.

[39] B. D. Cullity, S. R. Stock, Elements of X-Ray Diffraction, third ed., Prentice-Hall, 2001, pp. 167-171.

[40] A.F. Mayadas, M. Shatzkes, Electrical-resistivity model for polycrystalline films: The case of arbitrary reflection at external surfaces, Phys. Rev. B. **1** (1970) 1382-1389.

[41] J.M.E. Harper, C. Cabral Jr., P.C. Andricacos, L. Gignac, I.C. Noyan, K.P. Rodbell, C.K. Hu, Mechanism for microstructure evolution in electroplated copper thin films near room temperature, J. Appl. Phys. **86** (1999) 2516-2525.

[42] X.H. Chen, L. Lu, K. Lu, Electrical resistivity of ultrafine-grained copper with nanoscale growth twins, J. Appl. Phys. **102** (2007) 083708.

[43] T. Osaka, N. Yamachika, M. Yoshino, M. Hasegawa, Y. Negishi, Y. Okinaka, Effect of carbon content on the electrical resistivity of electrodeposited copper, Electrochem. Solid-State Lett. **12** (2009) D15-D17.

[44] E.O. Hall, The deformation and ageing of mild steel: III Discussion of Results, Proc. Phys. Soc., London, **64** (1951) 747-753. N.J. Petch, The cleavage strength of polycrystals, J. Iron Steel Inst. London, **173** (1953) 25-28.

[45] J.R. Davis, ASM Speciality Handbook: Copper and Copper Alloys, ASM International, Materials Park, OH, 2001.

[46] E.M. Hofer, H.E. Hintermann, The structure of electrodeposited copper examined by x-ray diffraction techniques, J. Electrochem. Soc. **112** (1965) 167-173.

[47] A. Ibanez, E. Fatas, Mechanical and structural properties of electrodeposited copper and their relation with the electrodeposition parameters, Surf. Coat. Technol. **191** (2005) 7-16.

[48] R. Manu, S. Jayakrishnan, Influence of polymer additive molecular weight on surface and microstructural characteristics of electrodeposited copper, Bull. Mater, Sci, **34** (2011) 347-356.

[49] T.P. Moffat, D. Wheeler, D. Josell, Superfilling and the curvature enhanced accelerator coverage mechanism, The Electrochemical Society *Interface*, Winter, 2004.

[50] N. Pewnim, S. Roy, Effect of fluorosurfactant additive during Cu-Sn codeposition from methanesulfonic acid, J. Electrochem. Soc., **162** (2015) D360-D364.

Figure captions

Figure 1: Unipolar waveform identifying the pulse parameters that can be varied independently: T_{on}, T_{off} and i_p. The pulse on-time, T_{on}, is the length of time a peak current, i_p, is imposed, while the pulse off-time, T_{off}, is the duration when the current is switched off.

Figure 2: SEM images of PC–plated copper deposits from electrolytes with different additive concentration: a) EP-0, b) EP-17, c) EP-33, d) EP-50, e) EP-100 w and f) EP-200; and standard electrolyte g) SP-0 with no additive and h) SP-100 with 100% additive. These percentages are relative to the industry recommended additive concentration of 10 ml/L Copper Gleam B, 0.5 ml/L Copper Gleam A, and 70 ppm Cl^-.

Figure 3: EBSD images of pulse deposited copper from EnFACE electrolyte with different additive concentration: : a) EP-17, b) EP-33, c) EP-50, d) EP-100, e) EP-200, and f) SP-100. These percentages are relative to the industry recommended additive concentration of 10 ml/L Copper Gleam B, 0.5 ml/L Copper Gleam A, and 70 ppm Cl^-. The calibration bar represents a length of 2 μm. The different colours in the EBSD map represent different crystals planes as described by the g) inverse pole legend.

Figure 4: Grain size of DC and PC-plated Cu using the EnFACE electrolyte at different additive concentrations. The open symbols represent the grain sizes for PC deposition and filled symbols denote those obtained by DC plating. The samples marked with “E-X” refer to the DC plated samples plated from the corresponding electrolyte E-XX.

Figure 5: XRD scans of (a) DC plated (b) PC plated copper films at different additive concentration. The scans were shifted along the intensity axis except the high concentration setting. The intensity of the peaks was not adjusted to reveal the true intensity.

Figure 6: Texture coefficient of a) (111) and b) (200) for DC and PC plated Cu films. A Tc value greater than 1 indicates preferred orientation for a plane.

Figure 7: The dependence of the resistivity, ρ_G on grain size for DC (■) and pulse plated (□) copper films. The solid line is the fit of eqn. (7) to the DC data with $R = 0.7$ and $\rho_0 = 2.15$ μΩ cm; the dotted line represents the fit to the pulse data with $R = 0.8$ and $\rho_0 = 2.0$ μΩ cm.

Figure 8: a) Yield strength, b) tensile strength and c) ductility of DC and PC-plated Cu using the EnFACE and standard electrolytes.

Figure 9: Comparison of the theoretical Hall-Petch equation and actual yield strength in PC and DC-plated from a Cu 0.1 M $CuSO_4$ solution with different additive concentration.

Tables

Table 1: Electrolyte compositions used for DC and PC electroplating experiments.

Electrolyte Designation*	Description	$CuSO_4$ (M)	H_2SO_4 (M)	Gleam B (ml/L)	Gleam A (ml/L)	HCl (ppm)
E-0	Additive-free, 0.1 M $CuSO_4$	0.10	x	x	x	x
E-17	17% of the recommended concentration	0.10	x	1.7	0.09	12
E-33	33% of the recommended concentration	0.10	x	3.3	0.17	23
E-50	50% of the recommended concentration	0.10	x	5.0	0.25	35
E-100	Recommended concentration	0.10	x	10	0.50	70
E-200	High concentration (double the recommended concentration)	0.10	x	20	1.0	140
S-100	Standard electrolyte	0.63	2.0	10	0.5	70
S-0	Standard w/o additives	0.63	2.0	x	x	x

*'XX' is a number that stands for the percentage of additive concentration added to the electrolyte.

Table 2: Parameters used for DC electrodeposition for different electrolytes.

Electrolyte	Limiting current density (mA cm^{-2})	Plating current density (mA cm^{-2})	Plating efficiency (%)	Plating time to obtain 25 μm deposit (min)
E-0	5.22	2.09	87	615
E-17	5.10	2.04	86	623
E-33	4.95	1.98	91	623
E-50	4.59	1.84	92	669
E-100	4.19	1.68	94	705
E-200	4.07	1.63	96	708
S	18.25	7.30	97	146
S-0	20.32	8.13	97	152

Table 3 Parameters used for pulse deposition.

Electrolyte	Pulse limiting current density (mA cm^{-2})	Plating current density (mA cm^{-2})	Plating efficiency (%)	Plating time to obtain 25 μm deposit (min)	N_m	N_p
EP-0	17.47	6.99	64	1022	0.33	0.40
EP-17	17.43	6.97	74	885	0.33	0.40
EP-33	16.31	6.52	77	909	0.33	0.40
EP-50	15.09	6.04	78	971	0.33	0.40
EP-100	13.84	5.54	85	971	0.33	0.40
EP-200	13.74	5.50	83	978	0.33	0.40

Table 4: Comparison of grain sizes of DC and PC-plated deposits

Electrolyte Used	DC-plated Cu grain size (nm) [26]	PC-plated Cu grain size (nm)
E-0	9016	2459
E-17	758	659
E-33	523	465
E-50	466	335
E-100	407	303
E-200	400	235
S-0	11524	8941
S-100	431	290

Table 5: Mechanical and Electrical Properties of DC and PC plated copper deposits.

Sample	**Resistivity ($\mu\Omega$ cm)**	**Tensile strength (MPa)**	**Ductility (%)**
E-50	2.39	213	2.09
EP-50	2.07	329	2.94
EP-33	2.05	309	3.08
IPC standard	2.00	207	3.00

Figures

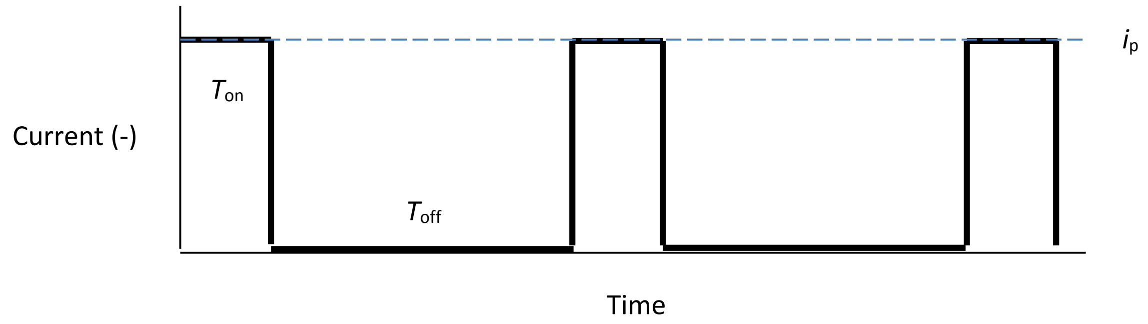

Figure 1

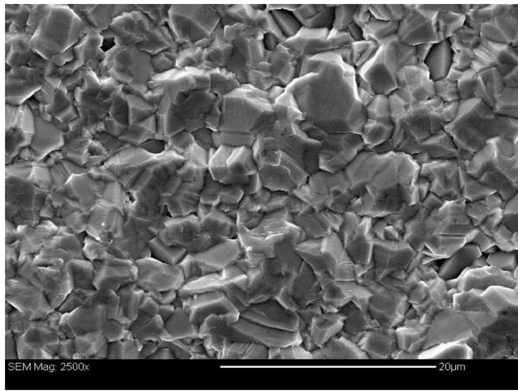

a) EP-0

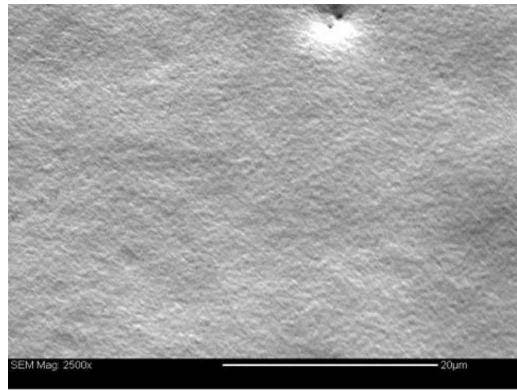

b) EP-17

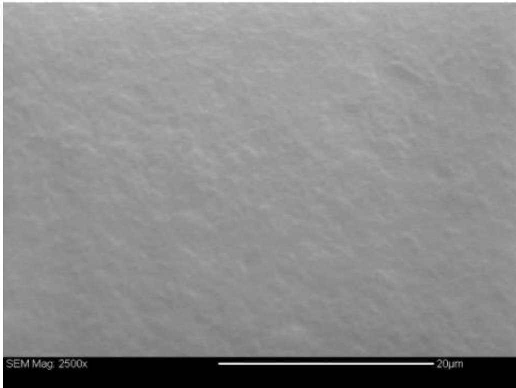

c) EP-33

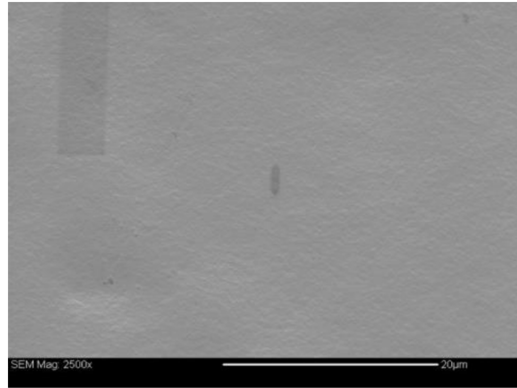

d) EP-50

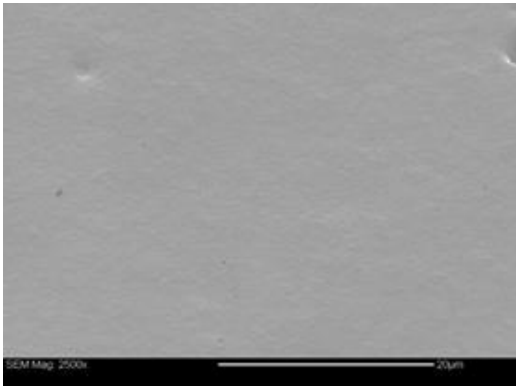

e) EP-100

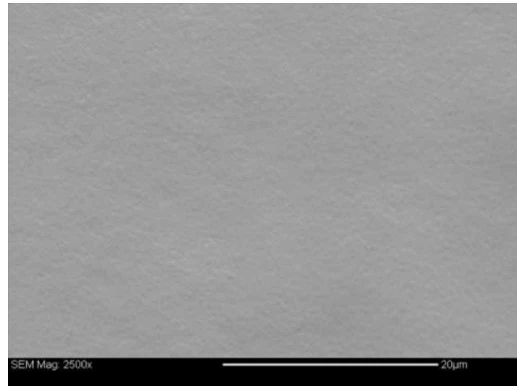

f) EP-200

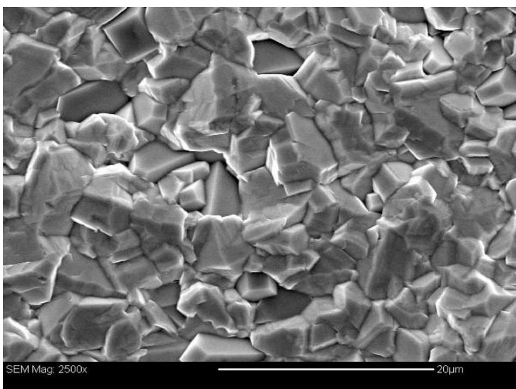

g) SP-0

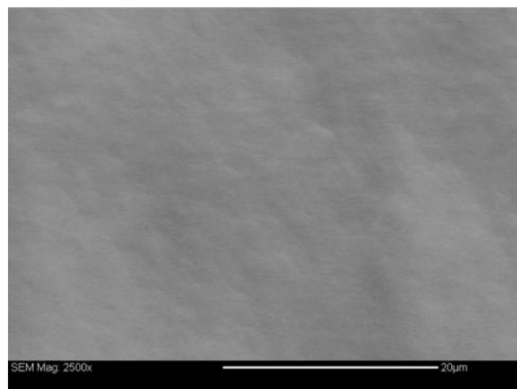

h) SP-100

Figure 2

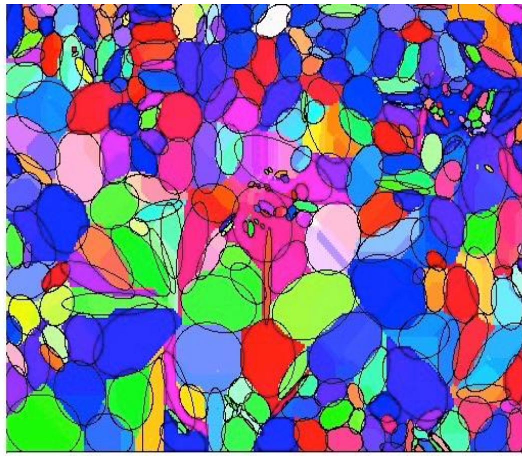

a) EP-17

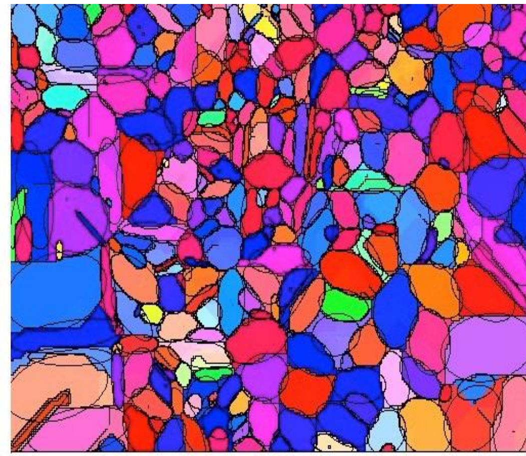

b) EP-33

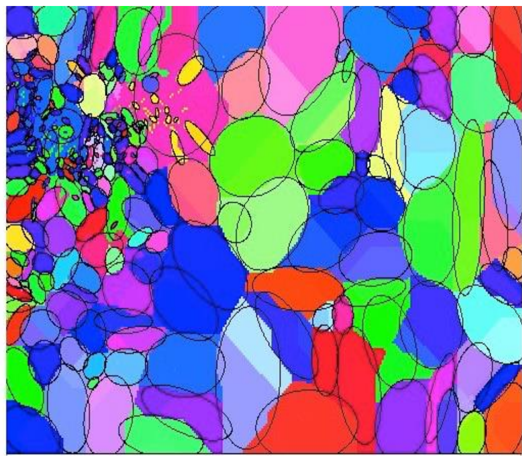

c) EP-50

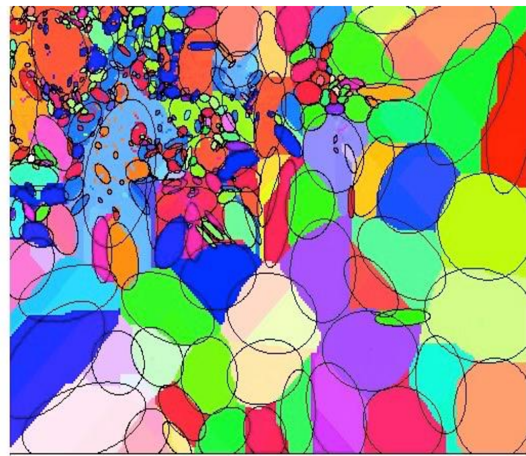

d) E-100/P

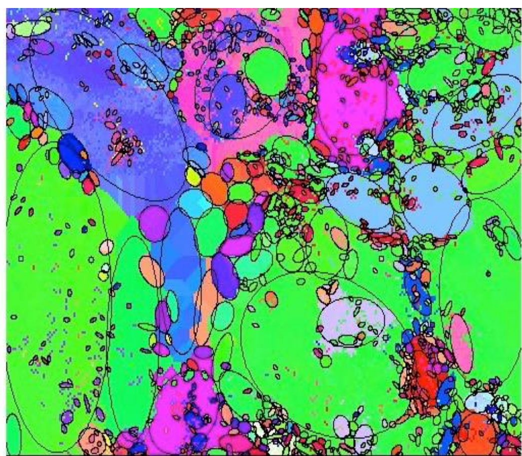

e) EP-200

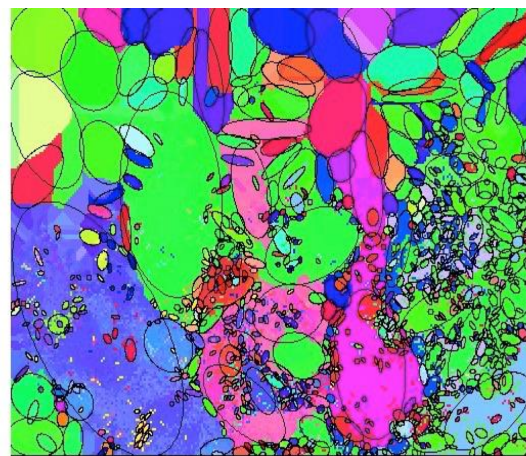

f) SP-100

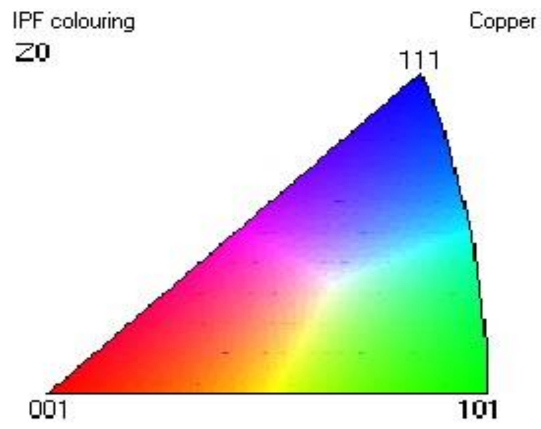

g) inverse pole legend

Figure 3

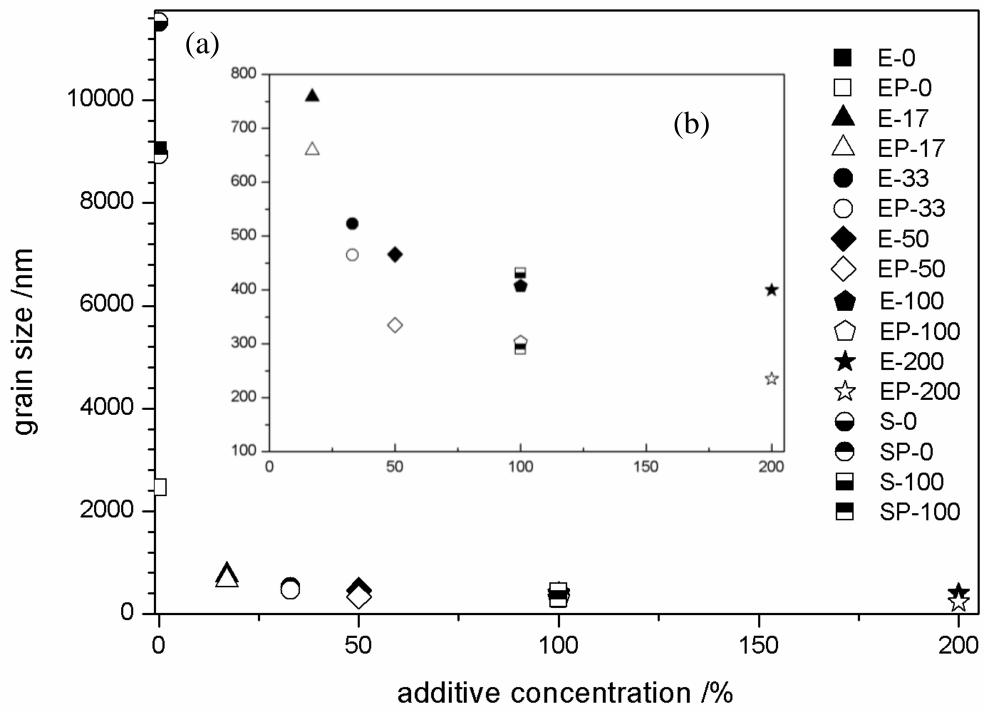

Figure 4

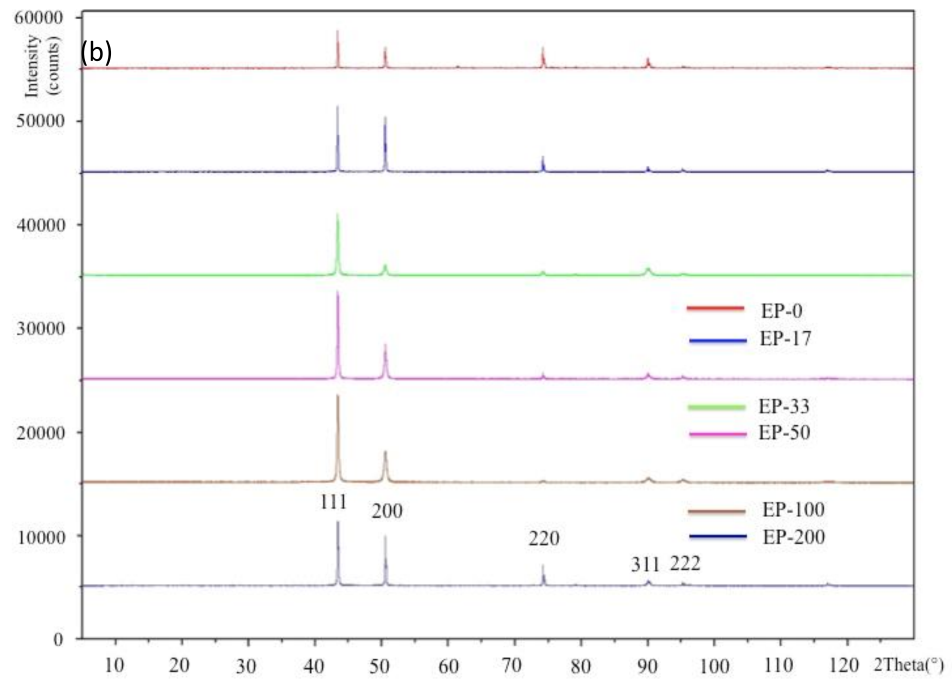

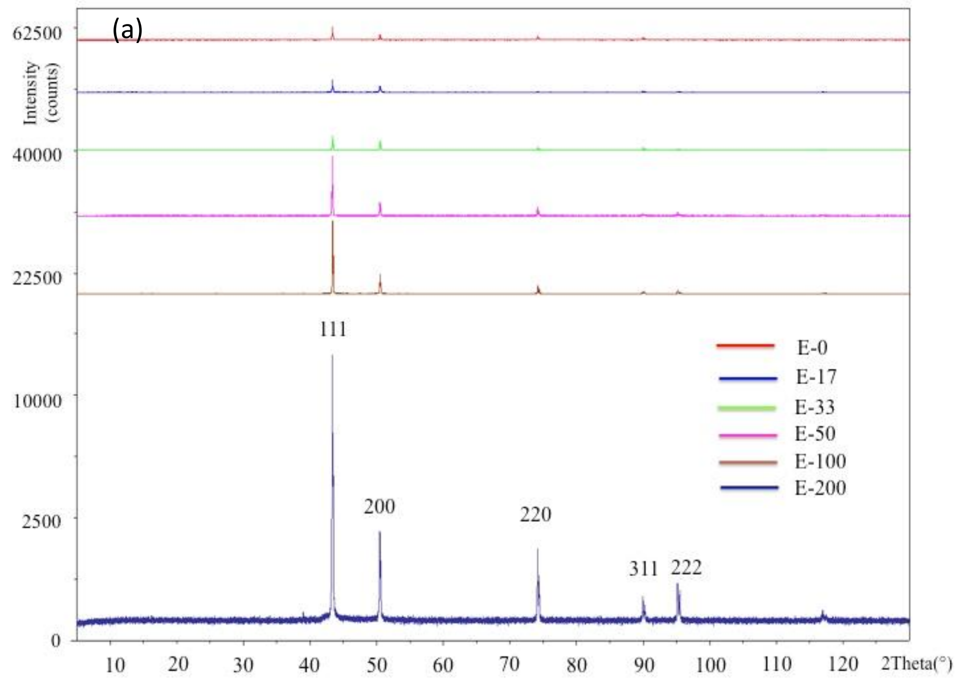

Figure 5

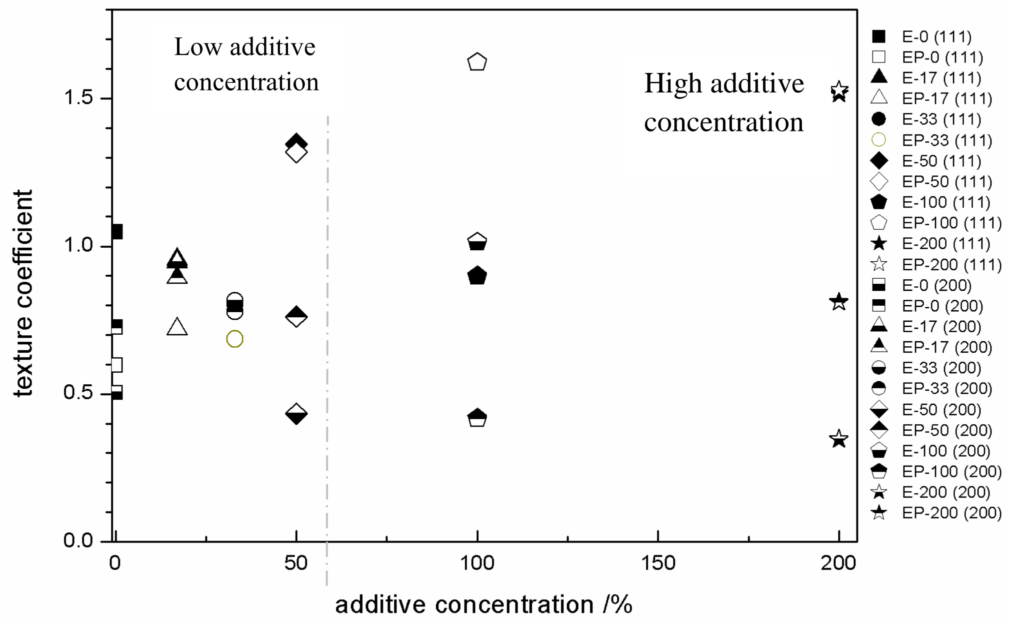

Figure 6

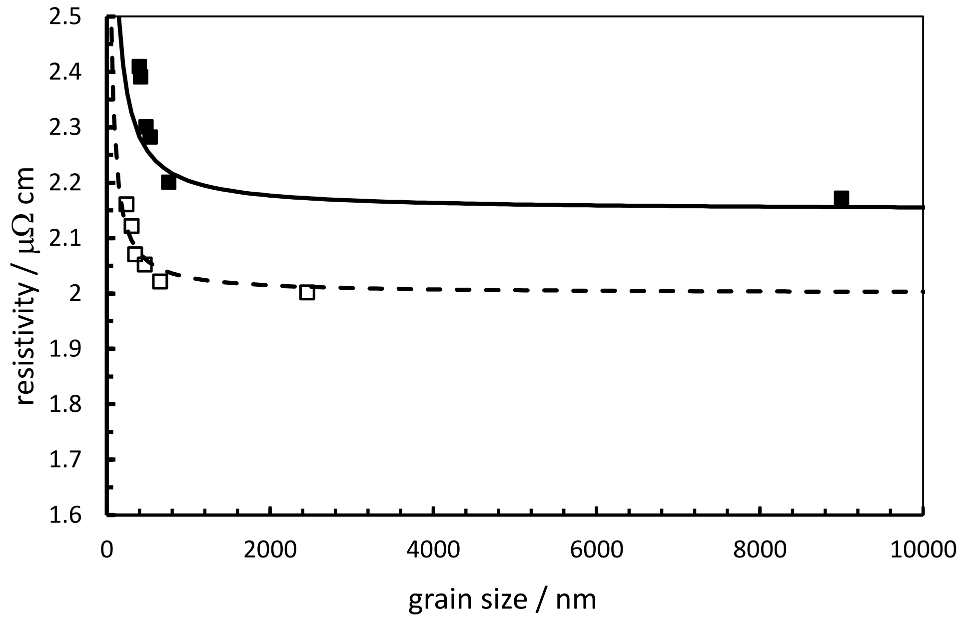

Figure 7

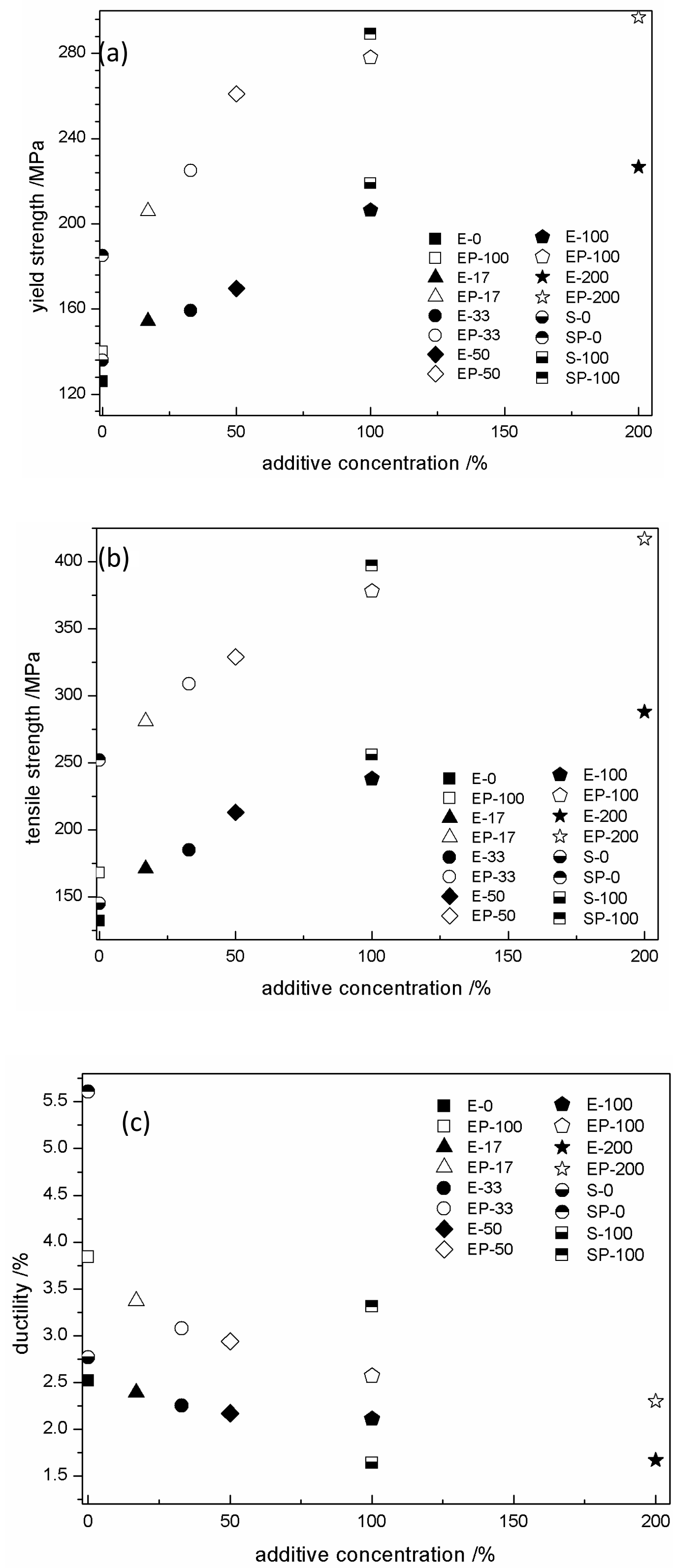

Figure 8

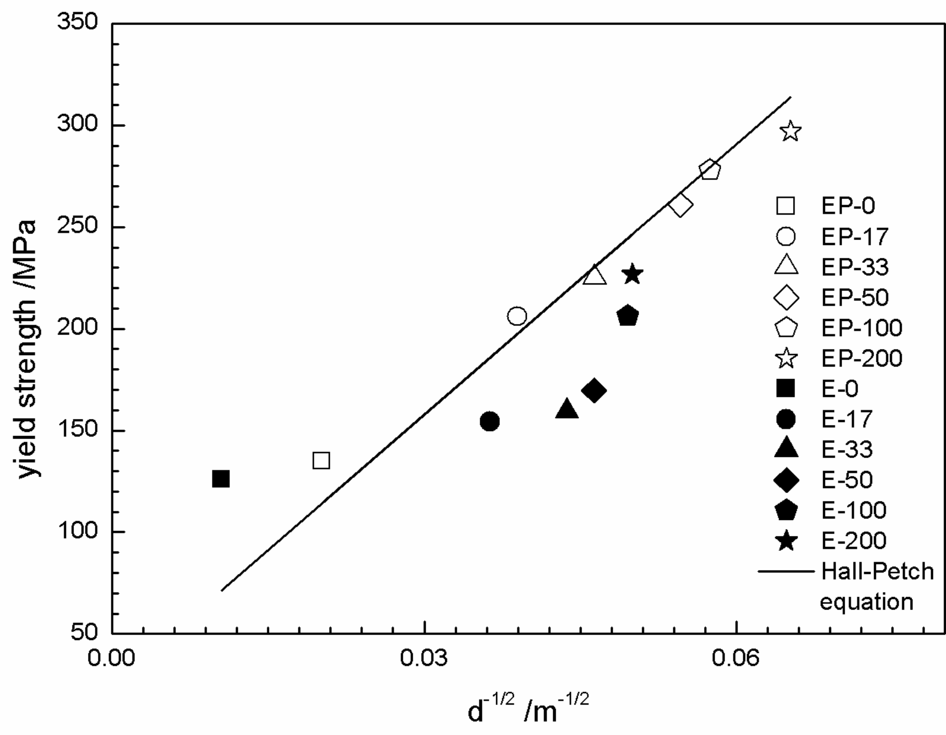

Figure 9